HHS Public Access

Author manuscript

Neuroimage. Author manuscript; available in PMC 2022 October 20.

Published in final edited form as:

Neuroimage. 2021 May 01; 231: 117850. doi:10.1016/j.neuroimage.2021.117850.

Higher-order sensorimotor circuit of the brain's global network supports human consciousness

Pengmin Qin[1,2,†,*], **Xuehai Wu**[3,4,5,†], **Changwei Wu**[6,7,8], **Hang Wu**[1], **Jun Zhang**[9], **Zirui Huang**[10], **Xuchu Weng**[11], **Zengxin Qi**[3], **Weijun Tang**[12], **Tanikawa Hiromi**[3], **Jiaxing Tan**[3], **Sean Tanabe**[10], **Stuart Fogel**[13], **Anthony G. Hudetz**[10], **Yihong Yang**[14], **Emmanuel A Stamatakis**[15], **Ying Mao**[3,*], **Georg Northoff**[16,17]

[1]Key Laboratory of Brain, Cognition and Education Sciences, Ministry of Education; School of Psychology, Center for Studies of Psychological Application, and Guangdong Key Laboratory of Mental Health and Cognitive Science, South China Normal University, Guangzhou, Guangdong, 510631, China

[2]Pazhou Lab, Guangzhou, 510335, China

[3]Department of Neurosurgery, Huashan Hospital, Shanghai Medical College, Fudan University, Shanghai, China.

[4]Neurosurgical Institute of Fudan University, Shanghai Clinical Medical Center of Neurosurgery, Shanghai Key laboratory of Brain Function Restoration and Neural Regeneration, Shanghai, China.

[5]State Key Laboratory of Medical Neurobiology and MOE Frontiers Center for Brain Science, School of Basic Medical Sciences and Institutes of Brain Science, Fudan University, Shanghai, China.

[6]Research Center for Brain and Consciousness, Taipei Medical University, Taipei, Taiwan.

[7]Graduate Institute of Humanities in Medicine, Taipei Medical University, Taipei, Taiwan.

[8]Shuang-Ho Hospital, Taipei Medical University, New Taipei, Taiwan.

[9]Department of Anesthesiology, Fudan University Shanghai Cancer center,Shanghai, China

[*]Correspondence to: Dr. Ying Mao, Neurosurgical Department, Shanghai Huashan Hospital, Fudan University, Shanghai, China, Phone: +86-13801769152, maoying@fudan.edu.cn, Dr. Pengmin Qin, Centre for Studies of Psychological Applications, Guangdong Key Laboratory of Mental Health and Cognitive Science, School of Psychology, South China Normal University, Guangzhou, Guangdong, China, Phone: +86 18665097531, qin.pengmin@m.scnu.edu.cn.

[†]These authors contributed equally to this work

Declaration of Competing Interest

None declared.

CRediT authorship contribution statement

Pengmin Qin: Conceptualization, Methodology, Formal analysis, Data Curation, Writing - Original Draft, Writing - Review & Editing, Visualization, Project administration, Funding acquisition. **Xuehai Wu:** Conceptualization, Methodology, Investigation, Writing - Review & Editing, Funding acquisition. **Changwei Wu:** Investigation. **Hang Wu:** Software, Formal analysis, Visualization. **Jun Zhang:** Investigation. **Zirui Huang:** Investigation. **Xuchu Weng:** Conceptualization. **Zengxin Qi:** Investigation. **Weijun Tang:** Investigation. **Tanikawa Hiromi:** Investigation. **Jiaxing Tan:** Investigation. **Sean Tanabe:** Investigation. **Stuart Fogel:** Investigation, Writing - Original Draft. **Anthony G. Hudetz:** Writing - Original Draft. **Yihong Yang:** Writing - Original Draft. **Emmanuel A Stamatakis:** Writing - Original Draft. **Ying Mao:** Conceptualization, Methodology, Writing - Review & Editing, Supervision. **Georg Northoff:** Conceptualization, Methodology, Writing - Original Draft, Writing - Review & Editing, Supervision, Funding acquisition.

[10]Department of Anesthesiology and Center for Consciousness Science, University of Michigan, Ann Arbor, MI, USA.

[11]Institute for Brain Research and Rehabilitation, South China Normal University, Guangzhou, Guangdong, China.

[12]Radiology Department, Shanghai Huashan Hospital, Fudan University, Shanghai, China.

[13]School of Psychology, University of Ottawa, Ottawa, Canada

[14]Neuroimaging Research Branch, National Institute on Drug Abuse, Intramural Research Programs, National Institutes of Health, Baltimore, USA

[15]Division of Anaesthesia, School of Clinical Medicine, University of Cambridge, Cambridge, UK.

[16]Institute of Mental Health Research, University of Ottawa, Ottawa, Ontario, Canada

[17]Mental Health Centre, Zhejiang University School of Medicine, Hangzhou, China

Abstract

Consciousness is the defining property of the mind, whose exact neural correlates in the brain's local and global activity remain unclear. We aimed to identify the critical nodes within the brain's global functional network that support consciousness. To that end, we leveraged a large fMRI resting state dataset obtained from subjects in three distinct states where consciousness was either preserved (healthy awake state), reduced (N1-sleep state, and minimally conscious state), or lost (N3-sleep state, anesthesia, and unresponsive wakefulness state). We included a unique dataset of subjects in rapid eye movement sleep state (REM-sleep) to test for the presence of consciousness during the absence of movements and sensory input. To identify critical nodes, i.e., hubs, within the brain's global functional network, we used a graph-theoretical measure of degree centrality conjoined with ROI-based functional connectivity of brain networks. We found that various higher-order sensory and motor regions including supplementary motor area, bilateral supramarginal gyrus (part of inferior parietal lobule), supragenual/dorsal anterior cingulate cortex, and left middle temporal gyrus were important hubs whose degree centrality was significantly reduced when consciousness remained absent (as observed in all groups). Additionally, we observed high degrees of functional connectivity among these regions, forming a sensorimotor circuit which was significantly correlated with levels of consciousness across the different groups and remained present in the REM-sleep group. Taken together, we demonstrate that regions forming a higher-order sensorimotor integration circuit are central in supporting consciousness within the brain's global functional network. That offers novel and more mechanism-guided treatment targets for disorders of consciousness.

Keywords

Anesthesia; Degree centrality; Inferior parietal lobule; rapid eye movement sleep; higher-order sensorimotor circuit; disorders of consciousness

1. Introduction

Consciousness is a core feature of the brain, and the neural correlates of consciousness (NCC) (Crick and Koch, 2003) have been the focus of intensive investigation in neuroscience (Bachmann, 2015; Koch et al., 2016; Tononi et al., 2016). Studies employing various methodologies including functional magnetic resonance imaging and multichannel electroencephalography so far have yielded conflicting views on whether resting state and task-evoked activity of specific sensory and cognitive brain regions such as the posterior "hot zone" (Koch et al., 2016) or the dorsolateral prefrontal cortex may serve as the NCC (Dehaene and Changeux, 2011). In addition to specific regions and regional specialization, the long-distance communication among remote brain regions as well as global activity changes have been emphasized (Huang et al., 2016; Luppi et al., 2019; Tanabe et al., 2020; Tang et al., 2017). Efforts have been directed to identifying the particular regions of the brain's global functional network, which in graph theoretical terms are called "hubs", may be critical in supporting consciousness. Hubs or nodes reflect local activity in specific regions that strongly modulate the brain's global activity (Boly et al., 2017). While recent approaches identified the dynamic nature of the NCC (Demertzi et al., 2019), the regions and circuit that support consciousness within the brain's global functional network remain yet unclear.

Insights into the NCC as a state have strongly benefited from investigations of abnormal behavioral and brain states characterized by reduced or absent consciousness, e.g., in anesthesia (Hashmi et al., 2017; Kertai et al., 2012; Monti et al., 2013; Moon et al., 2015), sleep (Horovitz et al., 2009; Houldin et al., 2019; Hu et al., 2020; Larson-Prior et al., 2009), unresponsive wakefulness syndrome (UWS) and minimally conscious state (MCS) (Engemann et al., 2018; Monti et al., 2010; Schiff, 2015). One particularly powerful approach is to identify brain regions and networks whose activity patterns could track the variations in the behaviorally defined states of consciousness.

Prior investigations, especially in UWS, have demonstrated abnormal activity in higher-order sensory and motor regions like supplementary motor area (SMA) (Owen et al., 2006) and inferior parietal lobule (IPL) (Zhang et al., 2018b), while the stimulus evoked activity of primary sensory regions is largely preserved (Di et al., 2007). These studies suggested that sensorimotor integration is required for normal, healthy consciousness (O'Regan and Noe, 2001). The findings highlighted a key role for a higher-order sensorimotor integration circuit in supporting consciousness. However, additional higher-order regions and functional networks like the salience network (Qin et al., 2015), default-mode network (Vanhaudenhuyse et al., 2010), and frontal-executive network (Stender et al., 2014) have also been implicated in states of reduced or absent consciousness. Some studies even suggest that the brain's global spatial activity pattern that operates across the whole brain may be central in supporting consciousness (Tanabe et al., 2020). Taken together findings on local and global activity changes, we are confronted with the question how local and global activity can be reconciled in their support for consciousness – that is the main focus of our study. Specifically, we asked whether consciousness is supported by the existence of a higher-order sensorimotor integration circuit within the brain's global functional network.

To address the above question, degree centrality (DC), a graph theoretical measure, is a useful tool. Based on the resting-state fMRI data, degree centrality allows measuring the relative importance and contributions of specific regions serving as nodes within the global overall network architecture by calculating the number of connections made to a node (voxel) (van den Heuvel and Sporns, 2013). This approach is suitable for calculating the degree of functional integration (centrality) of hubs in a complex network such as the brain. Brain regions with high degree centrality and their functional connections are thought to allow for higher-order integration of different inputs like sensory and motor, i.e., higher-order sensorimotor integration (Bullmore and Sporns, 2012).

In this study, we aim to identify the higher-order integration nodes forming a circuit within the brain's global functional network using resting-state fMRI. Importantly, we aim to show how such circuit can track behaviorally defined states of consciousness from normal wakefulness to pharmacological and neuropathological states where consciousness was presumed to be reduced or lost. We take advantage of a large dataset that included subjects in anesthesia, sleep, and patients with disorders of consciousness (DOC, including UWS and MCS). Most importantly, we also include a unique fMRI dataset on REM-sleep, where sensory input is maximally reduced and the ability of intentional movement generation/execution is lost while the subjects still maintain rich conscious experiences. Investigating REM-sleep will thus provide a unique window into understanding the NCC by itself, independent of sensory and motor processing. This is particularly important because REM-sleep will be helpful to exclude the possibility of effects caused by a lack of mobility, since unconscious states are also characterized by immobility (e.g. sleep, anesthesia, and UWS). REM-sleep on the other hand, also helps excluding the possibility of effects caused by a lack of environmental sensory inputs, since REM-sleep and unconscious states share the same disconnection from the external world.

Specifically, the present study is divided into two parts. The first part is exploratory and involves a sleep group without REM (including awake state, N1-sleep, and N3-sleep), an anesthesia group (including conscious wake and anesthesia states), and DOC patients (including UWS, MCS and a fully conscious patient group with brain lesions (BL)) (See Supplementary Table 1). All DOC patients were structurally preserved brain injury patients (Supplementary fig. 1 for structural brain images). For the sleep group, N3-sleep was regarded as an unconscious state (deep sleep stage) (Laureys, 2005). The second part of our study focuses on validation of the regions obtained in the first part by involving a REM-sleep group (including awake, N3-sleep and REM-sleep). For the data-analysis, during the first exploratory part, the brain regions with significant degree centrality reduction during unconsciousness were discovered, and then further confirmed with the REM-sleep dataset. The functional connections between each of these brain regions were investigated in all levels ranging from consciousness to unconsciousness; that served the purpose to extract the functionally relevant circuit among different regions within the global functional network. Please see Fig. 1 for the main idea of the manuscript and the Schemata of data processing.

2. Materials and Methods

2.1 Participants and data acquisition – Sleep group

This dataset is from a previously published study (Tsai et al., 2014). There were 12 healthy men with regular sleep duration of 7–8 h per night and consistent bed/wake time for at least 4 days. Participants' age ranged from 20 to 27 years (mean ± SD = 23 ± 2.5 years). We conducted simultaneous EEG–fMRI recordings for the sleep protocol. EEG was recorded using a 32-channel MR-compatible system (Brain Products, Gilching, Germany). The 32 electrodes, including 30 EEG channels, one electrooculography (EOG) channel, and one electrocardiogram (ECG) channel, were positioned according to the international 10/20 system. The electrode-skin impedance was reduced to <5 kΩ using abrasive electrode paste (ABRALYT HiCl). The EEG signal was synchronized with the MR trigger and recorded using the Brain Vision Recorder software (Brain Products) with a 5 kHz sampling rate and a 0.1 μV voltage resolution. Low-pass and high-pass filters were set at 250 Hz and 0.0159 Hz, respectively, with an additional 60-Hz notch filter.

The sleep protocol was conducted at midnight and the participants were instructed to try to fall asleep after the EPI scan started. A licensed sleep technician in Kaohsiung Medical University Hospital visually scored the sleep stages for every 30 s epoch, according to the current criteria of the American Academy of Sleep Medicine (AASM). In the current study, the awake state (before sleep), N1-sleep, and N3-sleep were included in the analysis. See the previous study for detailed information about the EEG and fMRI data acquisition parameters and data preprocessing (Tsai et al., 2014).

2,2 Participants and data acquisition – REM-Sleep group

These datasets were from a previously published study (Fang et al., 2019) using simultaneous EEG–fMRI recordings. There were 24 healthy participants (age from 18 years to 34 years, mean ± SD = 23.8 ± 4.1 years, 9 female) included in the current analysis. The awake-state was recorded in 19 participants (which occurred during sleep, not before sleep), the N3-state was recorded in 11 participants and the REM-sleep was recorded in seven participants. One participant had all of the awake, N3-sleep and REM-sleep states; two participants had both the N3-sleep and REM-sleep; two participants had both the awake and REM-sleep; seven participants had both the awake and N3-sleep. Each sleep state had a minimum of 90 volumes. The sleep stages were scored in the same way as sleep group 1. See the previous study for detailed information about the EEG and fMRI data acquisition parameters and data preprocessing (Fang et al., 2019).

2.3 Participants and data acquisition – Anesthesia group

Seventeen participants received intravenous propofol anesthesia and six subjects received inhalational sevoflurane anesthesia. The participants' age ranged from 26 years to 63 years (mean ± SD = 45.8 ± 11.8 years, 11 female). All the subjects had received the elective transsphenoidal approach for resection of pituitary microadenoma. Informed written consent was obtained from each subject. The study was approved by the Ethics Committee of Shanghai Huashan Hospital, Fudan University, Shanghai, China.

For the propofol group, we achieved a 3.0–5.0 μg/ml plasma concentration by using a target-controlled infusion (TCI) based on the Marsh model. This was followed by remifentanil (1.0 μg/kg) and succinylcholine (1 mg/kg) to facilitate endotracheal intubation. We then maintained the TCI propofol at a stable effect-site concentration (4.0 μg/ml) which reliably induced an unconscious state in the subjects. For the sevoflurane group, we gave the subjects 8% sevoflurane in 100% oxygen, adjusting fresh gas flow to 6 L/min, combined with remifentanil (1.0 μg/kg) and succinylcholine (1.0 mg/kg). This was maintained with 2.6% (1.3 MAC) ETsevo in 100% oxygen, and a fresh gas flow at 2.0 L/min. The concentration of sevoflurane successfully maintained a loss of consciousness in subjects, classified as ASA physical status I or II (Katoh and Ikeda, 1998). The anesthetic effects on the brain are considered to be solely pertaining to propofol and sevoflurane because of the quick elimination of the analgesic remifentanil and depolarized neuromuscular relaxant succinylcholine from plasma. To confirm the effects of each drug, the results for each drug were also presented separately in the supplementary materials.

During the anesthetic state, subjects were given intermittent positive pressure ventilation, with tidal volume at 8–10 ml/kg, respiratory rate at 10–12 beats per minute, and $PetCO_2$ (end tidal partial pressure of CO_2) at 35–37 mmHg. All subjects met the criteria of deep sedation: neither a response to verbal commands (“squeeze my hand”), nor a response to prodding or shaking was observed during anesthesia, corresponding to Ramsay 5–6 and an OAA/S score of 1. In addition, no subject reported explicit memory in the post-operative follow-up. Therefore, all subjects were considered unconscious during anesthesia. See the previous study for the detailed information of the anesthesia protocols (Huang et al., 2016; Zhang et al., 2018a).

All the datasets had the same fMRI acquisition parameters. A Siemens 3T scanner used T2*-weighted EPI sequence to acquire functional images of the whole brain (TR/TE/θ= 2000ms/30 ms/90°, FOV = 192 mm, matrix size = 64 × 64, 25 slices with 6-mm thickness, gap = 0 mm, 240 scans). A high-resolution T1-weighted anatomical image was also acquired for all participants. EPI data acquisition was conducted both in wakefulness prior to anesthesia and in the anaesthetized state. The subjects were instructed to relax and keep their eyes closed during scanning. Following this, subjects were anaesthetized and given full hydration with hydroxyethyl starch to avoid hypotension. The anaesthetized state resting-state fMRI scan was performed fifteen minutes after stabilization of anaesthetic levels and hemodynamics.

2.4 Participants and data acquisition –patients with disorders of consciousness

To minimize the effects of structural distortion and maintain local neural integrity for the degree centrality analysis, we included 50 structurally well-preserved brain injury patients with three different conditions: UWS, MCS and BL. These structurally well-preserved patients, who were selected by author XW and then checked by author PQ according to their structural images, had limited brain lesions and limited brain structure distortion (Supplementary Table 1 for detailed demographic and clinical information, and Supplementary fig. 1 for each patient’s structural image). The UWS and MCS patients were assessed using the Coma Recovery Scale-Revised (CRS-R) (Giacino et al., 2004)

before the fMRI scanning. Informed written consent was obtained from the patients' legal representatives. The study was approved by the Ethics Committee of Shanghai Huashan Hospital, Fudan University, Shanghai, China.

For the datasets in the current study, the MR images were acquired on the same Siemens 3 Tesla scanner. Functional images were acquired using a T2*-weighted EPI sequence (TR/TE/θ = 2000 ms/35 ms/90°, FOV = 256 × 256 mm, matrix= 64 × 64, 33 slices with 4-mm thickness, gap = 0 mm, 200 scans). Each volume had 33 axial slices, covering the whole brain. Two hundred volumes were acquired during rest. A high-resolution T1-weighted anatomical image was acquired for all participants for functional image registration and localization. The patients were instructed to take a comfortable supine position, relax, close their eyes, and not concentrate on anything in particular during the scanning. All participants wore earplugs to minimize the noise of the scanner.

2.5 Data preprocessing

Anatomical images from the two sleep groups, anesthesia, and patient with DOC were segmented into grey matter (GM), white matter (WM), and cerebrospinal fluid (CSF), using the FAST tool from the FSL software package (http://www.fmrib.ox.ac.uk/fsl/). Functional images were processed using the AFNI software package. After discarding the first two volumes, functional images underwent a preprocessing procedure which included: slice-timing correction; head-motion correction; masking for the removal of the skull; and spatial smoothing using an 8-mm kernel. Time-series were then intensity normalized by computing the ratio of the signal in each voxel at each time point to the mean across all time points, and then multiplied by 100. The six estimated head motion parameters and the mean time-series from the white matter (WM) and the cerebrospinal fluid (CSF), which were defined using partial volume thresholds of 0.99 for each tissue type, were considered as noise covariates and were regressed out from the data. The data were band-pass filtered preserving signals between 0.01 and 0.08 Hz. Functional images from all the three groups were transformed into MNI standard space ($3 \times 3 \times 3$ mm^3 resolution).

For all the datasets, the issue of head motion was rigorously addressed, as minor differences in motion have been shown to cause artificial group differences (Power et al., 2012). Motion was quantified as the Euclidean distance calculated from the six rigid-body motion parameters for two consecutive time points (AFNI, 1d_tool.py). Any instance of movement greater than 0.5 mm was considered as excessive, for which the respective volume as well as the immediately preceding and subsequent volumes were removed. In order to obtain reliable results, participants with less than 90 scans remaining were excluded (Yan et al., 2013).

2.6 Degree centrality changes in different conscious levels

For the sleep group, the REM-sleep group, anesthesia, and DOC patients, voxel-wise degree centrality analysis was performed within a grey matter mask (Yeo et al., 2011) using the AFNI program 3dTcorrMap. In the current analysis, each voxel constitutes a node, and each functional connection (Pearson correlation at $r > 0.3$) between the node and any other voxel (node) within the grey matter mask constitutes an edge. Degree centrality counts the number

of edges connecting to a node. We hereby adopted different thresholds (Pearson correlation at $r > 0.2$ and $r > 0.4$) for validation.

For the sleep group, awake and N1-sleep were regarded as consciousness or reduced consciousness states while N3-sleep as an unconscious state (Laureys, 2005); for the anesthesia group, awake consciousness was the conscious state while anesthetic state was an unconscious state. For the DOC group, the BL and MCS were regarded as consciousness or reduced consciousness states while UWS as an unconscious state. For REM-sleep group, the awake and REM-sleep were regarded as consciousness or reduced consciousness states while N3-sleep as unconscious state.

In order to identify the common brain regions with degree centrality changes during unconscious states, paired t-tests were performed to compare voxel-wise differences between unconscious and conscious states for the anesthesia group. For the sleep group, repeated measures ANOVA was applied to analyze the difference of degree centrality values between unconscious and conscious/reduced conscious states with the AFNI program (3dMVM). For the DOC group, ANCOVA was applied to analyze the voxel-wise contrasts of degree centrality values using the 3dMVM program in AFNI, in which age, gender, head motion, the length of time since brain injury, and the length of BOLD signal series were regarded as covariates. All tests above were two-tailed. For all these contrasts, a cluster-level significance threshold of $p < 0.05$ after FWE correction ($p < 0.005$ uncorrected, cluster size > 20 voxels, 3dClusterSim, AFNI) was used. The common brain regions with degree centrality reduction during unconsciousness detected in the anesthesia group, sleep group and DOC group were defined as the brain hubs (volume > 20 voxels).

For each common brain region with degree centrality reduction during unconsciousness in the sleep group, anesthesia group and DOC group, the coordinates of cluster centers were used to make ROIs (sphere with r = 8mm). Then for the REM-sleep group, mean degree centrality values within these ROIs were computed, respectively. For each ROI, the Kruskal-Wallis H test was applied to analyze the contrasts of degree centrality values; post-hoc test included: N3-sleep vs. REM-sleep, N3-sleep vs. Awake, and REM-sleep vs. awake. All tests above were two-tailed. The effect size was estimated using η_H^2. The FDR correction was used to control for the multiple comparison problem across all post-hoc tests among the five brain regions in the REM-sleep group.

2.7 Functional connectivity changes between brain regions with decreased degree centrality during unconscious states

Following the degree centrality analysis, ROI-based functional connectivity was performed with the ROIs obtained from the above analysis which showed degree centrality reduction in unconsciousness. Mean time-series from each region was calculated, and then the Pearson correlation coefficient was computed for each pair of regions. Fisher's Z transformation was used to transform the correlation r-values to normally distributed Z-values, which were then compared between unconscious and conscious states. In order to determine whether the functional connectivity of all the five regions was significant during consciousness or awake-states within each group, one-sample t-tests were applied to compare their Z-

values to 0.3095 (r value = 0.3). To test whether the relationship among all the pairs of functional connectivity was consistent during consciousness states, the correlations between the functional connectivity z-values during consciousness or awake states from one group and the values during the consciousness states from other groups were calculated using the Spearman's correlation. The p-value of the correlation coefficient were FDR corrected.

Additionally, the relationship between the mean functional connectivity z-value among all the pairs of ROI connections and levels of consciousness states were investigated in the sleep group, DOC group and REM-sleep group using the Spearman's correlation. Similar as the mean strength of functional connectivity, if the functional connectivity with a z-value (> 0.3095) was regarded as an edge, the relationship between the total edge number among the five brain regions and levels of consciousness was also investigated using Spearman's correlation. The p-value were FDR corrected. The anesthesia group was not included in this correlation analysis since it only included two levels of consciousness.

Finally, to determine the functional connectivity changes from consciousness to unconsciousness, the Wilcoxon rank-sum test was performed for each pair of ROIs in the anesthesia group. The FDR correction was adopted for all pairs of ROIs in the anesthesia group. For the sleep group, the Friedman's test was performed to compare the functional connectivity between each pair of ROIs among awake, N1-sleep, and N3-sleep. The FDR correction was adopted for all the post-hoc tests in the sleep group. For patients with DOC, the Kruskal-Wallis H test was applied to analyze the functional connectivity between each pair of ROIs among the UWS, MCS, and BL. The FDR correction was adopted for all the post-hoc tests in the DOC group. For the REM-sleep group, the Kruskal-Wallis H test was also applied to analyze the functional connectivity between each pair of ROIs in the N3-sleep, REM-sleep and awake group. Furthermore, the post-hoc test p-values of the REM-sleep group were corrected using the FDR correction. All the tests above were two-tailed. For all the statistics, degree centrality values or functional connectivity values beyond the range (mean±2SD) of each group were excluded.

3. Results

3.1 Reduced degree centrality in unconsciousness

As a first step, whole brain voxel-wise degree centrality analysis was performed to build a degree centrality map (r > 0.3 was taken as one edge). All the contrasts between conscious/reduced-conscious states and unconscious states showed brain regions with significant degree centrality reduction during unconscious states ($p < 0.05$ FWE correction), which overlapped in the supplementary motor area (SMA), the left supramarginal gyrus (LSMG), the right supramarginal gyrus (RSMG), the supragenual anterior cingulate cortex (SACC) and the left middle temporal gyrus (LMTG) among the sleep, anesthesia and DOC groups (Fig. 2 and supplementary Table 2). These five regions did not show any degree centrality difference between N1-sleep and awake-states in the sleep group. LSMG showed significant differences between BL and MCS, but not other four regions (Supplementary fig. 2).

3.2 Intact degree centrality in REM-sleep

The above five regions identified (SMA, SACC, bilateral SMG, and LMTG) were used as ROIs in REM-sleep datasets to test whether their degree centrality would be significantly reduced during N3-sleep, and intact during REM-sleep. There were three regions (SACC, SMA and LMTG) that showed a significant reduction of degree centrality during N3-sleep compared with REM-sleep and awake state. Both LSMG and RSMG showed significantly reduced degree centrality during N3-sleep compared with REM-sleep, and this difference was marginally significant between N3-sleep and awake (Fig. 3). We also validated the above findings by performing degree centrality analysis with different edge thresholds ($r > 0.2$ and $r > 0.4$) (Dai et al., 2015). Our results showed that all findings remained consistent when using different thresholds (Supplementary fig. 3).

3.3 ROI-based functional connectivity during consciousness

To reveal the connectivity of each pair of regions among the five brain regions, as well as to identify which connectivity showed reduction during unconsciousness, ROI-based functional connectivity was performed for all the states in all the four groups. The results showed that all five regions had significant functional connectivity ($z > 0.3095$) during consciousness or awake-state within each group, except the functional connectivity of LMTG with SMA and SACC in the anesthesia group. More interestingly, the strengths of the functional connectivity showed significant correlations between each pair of groups during consciousness or awake-states (Fig. 4 and Supplementary fig. 4). These results indicated that the functional connectivity between each pair of regions, as well as its relationship with other functional connectivity, was stable during consciousness. Please see the functional connectivity values of the five regions in reduced consciousness and unconsciousness in Supplementary fig. 5

3.4 The relationship between functional connectivity and levels of consciousness

The mean functional connectivity z-value among the five regions was significantly correlated with levels of consciousness states in the sleep group ($\rho = 0.69$, $p < 0.01$), DOC group ($\rho = 0.79$, $p < 0.01$), and REM-sleep group ($\rho = 0.48$, $p < 0.01$). Similar as the mean strength of functional connectivity, if the functional connectivity with a z-value (> 0.3095) was regarded as an edge, the total edge number among the five brain regions also showed a significant correlation in the sleep group ($\rho = 0.78$, $p < 0.01$), DOC group ($\rho = 0.81$, $p < 0.01$), and REM-sleep group ($\rho = 0.59$, $p < 0.01$) (Fig. 5). All the above p values were FDR corrected.

3.5 Specific functional connectivity which reduced during unconscious states

Comparing the functional connectivity of each pair of regions between consciousness and unconsciousness states, the functional connectivity between SMA and bilateral SMG, the functional connectivity between SACC and LSMG, the functional connectivity between SACC and LMTG, as well as the functional connectivity between bilateral SMG, showed a significant reduction in the unconsciousness state for all groups (Fig. 6). This result was further confirmed by voxel-wise analysis using the five ROIs (SMA, SACC, bilateral SMG and LMTG) as seeds (Fig. 7). Additionally, within the above the functional connectivity

with significant reduction during unconsciousness, the functional connectivity between SACC and LSMG, the functional connectivity between SACC and LMTG, as well as the functional connectivity between bilateral SMG, were significantly reduced in MCS compared with BL in the DOC group. But there was no functional connectivity which showed significant reduction in the N1-sleep or REM-sleep compared with awake state (Supplementary fig.6).

4. Discussion

In this study, we employed a graph-theoretical measure, i.e., degree centrality, and functional connectivity analysis to investigate the hubs in the brain's resting state that support consciousness. Degree centrality reflects the connections of one node with all other nodes throughout the brain. Our results revealed a reduced degree centrality in SMA, SACC, bilateral SMG and LMTG in the unconscious states (N3-sleep, anesthesia, and UWS) compared with the conscious and altered/partially conscious states (N1-sleep, MCS and REM-sleep).

Furthermore, functional connectivity analysis demonstrated that the connections among these five regions were significantly reduced during these unconscious states. Most interestingly, we found that this higher-order sensorimotor integration circuit was fully present in the REM-sleep, showing no difference compared with the awake states while exhibiting significant difference compared with the N3-sleep. This excludes sensory and motor input processing (as both are minimum in REM-sleep) as possible confounds of the higher-order sensorimotor integration circuit as the neural basis of consciousness. Therefore, we conclude that regions forming a higher-order sensorimotor integration circuit are central in supporting consciousness through their role as hubs within the brain's global functional network.

During the REM-sleep, one loses the ability of movement and sensory inputs from the external world. Most interestingly, similar as the REM-sleep, one type of patients named as cognitive motor dissociation (CMD) (Schiff, 2015), shows signs of consciousness with command-following brain activation but no detectable behavioral response (Monti et al., 2010). In the previous literatures, using motor imagery tasks, task-related activation in SMA can be used to identify CMD patients (Owen et al., 2006). However, the difficulty of such tasks and the cooperation of patients could lead to false negatives in the detection of CMD (Pan et al., 2020). Although the brain computer interface (BCI) provides another way to detect the CMD patients using face detection tasks (Pan et al., 2020), the current results may provide a much easier way to identify the CMD patients by using resting-state fMRI dataset without including any active tasks.

Furthermore, previous studies demonstrated global changes of degree centrality during unconsciousness (Hashmi et al., 2017; Tagliazucchi et al., 2013b). Our results extend these findings by showing significantly decreased degree centrality in specific brain regions: the SMA, SACC, bilateral SMG, LMTG in the unconscious states compared with the conscious and altered conscious states across all groups. All these five regions showed high degree centrality in the healthy conscious brain in previous studies (van den Heuvel and Sporns,

2013). Regions with high degree centrality enable efficient communication, and therefore information integration in a global way (van den Heuvel and Sporns, 2013). Consequently, the reduction in the degree centrality in these regions during unconsciousness possibly indicates their role in supporting consciousness within the brain's global functional network.

Our findings on the relationship between SMA and conscious processing are supported by previous studies in both fully conscious and unconscious subjects. The SMA has been shown to be involved in conscious processing in a variety of different tasks requiring sensorimotor integration. For instance, one study found that suppressing brain activity in the SMA affected visual perception (Martin-Signes et al., 2019). Using the subject's own name as stimulus, MCS patients showed stronger SMA response to their own names than UWS patients (Qin et al., 2010). SACC is another region involved in motor initiation, in which damages can result in akinetic mutism (Boly et al., 2017). SACC is also a core region of the salience network (Seeley et al., 2007), which shows altered activation during anesthesia (Huang et al., 2014), sleep (Mitra et al., 2015), and brain injury (Mitra et al., 2015; Qin et al., 2015). Our previous study showed the functional connectivity between the SACC and insula was correlated with the consciousness levels in DOC patients (Qin et al., 2015). This was consistent with the voxel-wise functional connectivity in the current study (Fig. 7).

Beside these motor regions, the SMG, a higher-order sensory region, showed a significant reduction of global integration during unconsciousness (Luppi et al., 2019). More importantly, the SMG is part of the inferior parietal lobule (IPL) which was reported to show reduced brain activations in the unconscious states (Lichtner et al., 2018). Since the IPL is close to the temporal and occipital cortices and receives both auditory and visual information (Dehaene and Changeux, 2011), and is involved in heartbeat awareness and body-centered perception (e.g., face and body) (Blanke et al., 2015), it is suggested to play a central role in integrating external and internal sensory information. Similar as the SMG, the LMTG was regarded as a part of the temporo-parietal-occipital hot zone, and was more related to content-specific neural correlates of consciousness in previous studies (Koch et al., 2016). Furthermore, the LMTG was also involved in the visual word detection task (Dehaene et al., 2001), and showed more activation during dreaming experience compared with no dreaming (Siclari et al., 2017).

More interestingly, the current results showed that the sum of functional connectivity (mean strength and edge) among these five regions was correlated with the levels of consciousness. This strongly suggests that they could form a circuit within the brain's global functional networks whose higher-order sensorimotor integration is key in supporting consciousness. Taken together, the reduced connectivity of these five regions suggests that the loss of consciousness may be contributed by a reduction in multiple high-order functional integrations, especially sensorimotor integration, which consistently showed reduction in all the unconscious states in the four groups.

The Default-mode network also showed reduced degree centrality in several contrasts between the conscious/altered conscious and unconscious states, such as the UWS (compared with MCS), as well as the anesthesia (compared with consciousness in anesthesia group), but not in all the contrasts between conscious/altered and unconscious states (Fig.

2). This was consistent with the previous studies. For instance, one study showed that the functional connectivity was correlated with levels of consciousness (Vanhaudenhuyse et al., 2010), while another study indicated that default-mode network was related to the recovery of consciousness, not the levels of consciousness (Norton et al., 2012).

Several issues should be noted. First, deep, surgical-level anesthesia was used, thus some of the anesthetic effects on the BOLD signal could be physiological in nature and unrelated to unconsciousness. In the current study, during the propofol-induced anesthesia in 17 participants, there was a significant reduction in the degree centrality in the SMA, SACC, bilateral SMG and LMTG during unconsciousness ($p < 0.05$ FDR corrected). Although there were only six participants receiving sevoflurane, their results also showed similar trends in all these regions, and a significant degree centrality reduction in the right SMG (See Supplementary fig. 7). Therefore, our results suggest that there are no major differences of degree centrality and functional connectivity between the two drugs. In the future, it may be useful to test other anesthetic drugs (e.g., ketamine) to confirm the current results. The second issue is that we did not specifically investigate dreams during both NREM and REM but took REM-sleep simply as an index of the presence of consciousness (Windt et al., 2016). Although different from wakefulness, the REM-sleep is considered a particular form of environmentally “disconnected” consciousness state (Tagliazucchi et al., 2013a). Here we not only showed the similarity of functional connectivity of the five brain hubs between a presumed dream state, i.e., REM, and the fully awake conscious state, but also its difference from that in the N3-sleep. Finally, our study included various datasets under different conditions, and the sample size for each individual dataset seems relatively small. However, the combined dataset for a specific analysis is sufficiently large. For instance, we collected two sleep datasets from two independent centers, and totally included 31 awake state and 23 N3-sleep state data, and the results of these two datasets were consistent with each other. Similarly, in the DOC dataset, the conscious state data included 27 patients with two groups (MCS and BL), whose contrasts with UWS showed the same pattern. All these indicated that our results were stable. Nevertheless, the sample size of the REM-sleep group with seven participants was small, even though the results were consistent with the other groups, and were supported by the previous literatures. In the future, more studies should be carried out to further confirm the current results.

5. Conclusions

In summary, we demonstrated that the SMA, SACC, bilateral SMG and LMTG participate in forming a higher-order sensorimotor integration circuit within the brain’s global functional network that supports consciousness. All these regions showed significant decreases in degree centrality and functional connectivity with each other during different unconscious conditions, i.e., anesthesia, N3-sleep, and patients with UWS. Furthermore, the mean strength and edge of functional connectivity of the five regions were significantly correlated with levels of consciousness. Interestingly, these properties were unchanged between wakefulness and REM-sleep. Based on their known functions in movement initiation and sensory information processing, we conclude that these regions could form a higher-order sensorimotor integration circuit that is essential for maintaining consciousness.

Supplementary Material

Refer to Web version on PubMed Central for supplementary material.

Acknowledgments

This work was sponsored by grants from Key Realm R&D Program of Guangzhou (202007030005 to PQ), the National Natural Science Foundation of China (Grant 31771249 to PQ; Grants 81571025 to XW), International Cooperation Project from Shanghai Science Foundation (No.18410711300 to Xuehai Wu), Shanghai Science and Technology Development funds (No. 16JC1420100 to Y.M), Shanghai Municipal Science and Technology Major Project (No.2018SHZDZX01 to Y.M), Natural Science Foundation and Major Basic Research Program of Shanghai (16JC1420100), Ministry of Science and Technology in Taiwan (MOST 105–2628-B-038–013-MY3), National Science Foundation of China (31471072), Taiwan Ministry of Science and Technology (105–2410-H-038–006-MY3, 105–2410-H-038–005-MY2); and Taipei Medical University (104–6402-006–110), and National Institute of General Medical Sciences of the National Institutes of Health (R01-GM103894, to AGH), Canadian Institutes of Health Research (CIHR), Michael Smith Foundation (EJLB-CIHR), The Hope for Depression Research Foundation (HDRF). This research project was also supported by the HBP Joint Platform to GN, funded from the European Union's Horizon 2020 Framework Program for research and Innovation under the specific Grant Agreement No 785907 (Human Brian Project SGA 2).

Data and materials availability

All data needed to evaluate the conclusions in the paper are present in the paper and the Supplementary Materials. Additional data related to this paper may be requested from the corresponding author.

Data and Code Availability Statement

All data needed to evaluate the conclusions in the paper are present in the paper and the Supplementary Materials. Additional data related to this paper may be requested from the corresponding author.

References

Bachmann T, 2015. On the brain-imaging markers of neural correlates of consciousness. Front Psychol 6, 868. [PubMed: 26161076]

Blanke O, Slater M, Serino A, 2015. Behavioral, Neural, and Computational Principles of Bodily Self-Consciousness. Neuron 88, 145–166. [PubMed: 26447578]

Boly M, Massimini M, Tsuchiya N, Postle BR, Koch C, Tononi G, 2017. Are the Neural Correlates of Consciousness in the Front or in the Back of the Cerebral Cortex? Clinical and Neuroimaging Evidence. J Neurosci 37, 9603–9613. [PubMed: 28978697]

Bullmore E, Sporns O, 2012. The economy of brain network organization. Nat Rev Neurosci 13, 336–349. [PubMed: 22498897]

Crick F, Koch C, 2003. A framework for consciousness. Nat Neurosci 6, 119–126. [PubMed: 12555104]

Dai Z, Yan C, Li K, Wang Z, Wang J, Cao M, Lin Q, Shu N, Xia M, Bi Y, He Y, 2015. Identifying and Mapping Connectivity Patterns of Brain Network Hubs in Alzheimer's Disease. Cereb Cortex 25, 3723–3742. [PubMed: 25331602]

Dehaene S, Changeux JP, 2011. Experimental and theoretical approaches to conscious processing. Neuron 70, 200–227. [PubMed: 21521609]

Dehaene S, Naccache L, Cohen L, Bihan DL, Mangin JF, Poline JB, Riviere D, 2001. Cerebral mechanisms of word masking and unconscious repetition priming. Nat Neurosci 4, 752–758. [PubMed: 11426233]

Demertzi A, Tagliazucchi E, Dehaene S, Deco G, Barttfeld P, Raimondo F, Martial C, Fernandez-Espejo D, Rohaut B, Voss HU, Schiff ND, Owen AM, Laureys S, Naccache L, Sitt JD, 2019. Human consciousness is supported by dynamic complex patterns of brain signal coordination. Sci Adv 5, eaat7603. [PubMed: 30775433]

Di HB, Yu SM, Weng XC, Laureys S, Yu D, Li JQ, Qin PM, Zhu YH, Zhang SZ, Chen YZ, 2007. Cerebral response to patient's own name in the vegetative and minimally conscious states. Neurology 68, 895–899. [PubMed: 17372124]

Engemann DA, Raimondo F, King JR, Rohaut B, Louppe G, Faugeras F, Annen J, Cassol H, Gosseries O, Fernandez-Slezak D, Laureys S, Naccache L, Dehaene S, Sitt JD, 2018. Robust EEG-based cross-site and cross-protocol classification of states of consciousness. Brain 141, 3179–3192. [PubMed: 30285102]

Fang Z, Ray LB, Owen AM, Fogel SM, 2019. Brain Activation Time-Locked to Sleep Spindles Associated With Human Cognitive Abilities. Front Neurosci 13, 46. [PubMed: 30787863]

Giacino JT, Kalmar K, Whyte J, 2004. The JFK Coma Recovery Scale-Revised: measurement characteristics and diagnostic utility. Arch Phys Med Rehabil 85, 2020–2029. [PubMed: 15605342]

Hashmi JA, Loggia ML, Khan S, Gao L, Kim J, Napadow V, Brown EN, Akeju O, 2017. Dexmedetomidine Disrupts the Local and Global Efficiencies of Large-scale Brain Networks. Anesthesiology 126, 419–430. [PubMed: 28092321]

Horovitz SG, Braun AR, Carr WS, Picchioni D, Balkin TJ, Fukunaga M, Duyn JH, 2009. Decoupling of the brain's default mode network during deep sleep. Proc Natl Acad Sci U S A 106, 11376–11381. [PubMed: 19549821]

Houldin E, Fang Z, Ray LB, Owen AM, Fogel SM, 2019. Toward a complete taxonomy of resting state networks across wakefulness and sleep: an assessment of spatially distinct resting state networks using independent component analysis. Sleep 42.

Hu X, Cheng LY, Chiu MH, Paller KA, 2020. Promoting memory consolidation during sleep: A meta-analysis of targeted memory reactivation. Psychol Bull 146, 218–244. [PubMed: 32027149]

Huang Z, Wang Z, Zhang J, Dai R, Wu J, Li Y, Liang W, Mao Y, Yang Z, Holland G, Zhang J, Northoff G, 2014. Altered temporal variance and neural synchronization of spontaneous brain activity in anesthesia. Hum Brain Mapp 35, 5368–5378. [PubMed: 24867379]

Huang Z, Zhang J, Wu J, Qin P, Wu X, Wang Z, Dai R, Li Y, Liang W, Mao Y, Yang Z, Zhang J, Wolff A, Northoff G, 2016. Decoupled temporal variability and signal synchronization of spontaneous brain activity in loss of consciousness: An fMRI study in anesthesia. Neuroimage 124, 693–703. [PubMed: 26343319]

Katoh T, Ikeda K, 1998. The effects of fentanyl on sevoflurane requirements for loss of consciousness and skin incision. Anesthesiology 88, 18–24. [PubMed: 9447851]

Kertai MD, Whitlock EL, Avidan MS, 2012. Brain monitoring with electroencephalography and the electroencephalogram-derived bispectral index during cardiac surgery. Anesth Analg 114, 533–546. [PubMed: 22253267]

Koch C, Massimini M, Boly M, Tononi G, 2016. Neural correlates of consciousness: progress and problems. Nat Rev Neurosci 17, 307–321. [PubMed: 27094080]

Larson-Prior LJ, Zempel JM, Nolan TS, Prior FW, Snyder AZ, Raichle ME, 2009. Cortical network functional connectivity in the descent to sleep. Proc Natl Acad Sci U S A 106, 4489–4494. [PubMed: 19255447]

Laureys S, 2005. The neural correlate of (un)awareness: lessons from the vegetative state. Trends Cogn Sci 9, 556–559. [PubMed: 16271507]

Lichtner G, Auksztulewicz R, Kirilina E, Velten H, Mavrodis D, Scheel M, Blankenburg F, von Dincklage F, 2018. Effects of propofol anesthesia on the processing of noxious stimuli in the spinal cord and the brain. Neuroimage 172, 642–653. [PubMed: 29421324]

Luppi AI, Craig MM, Pappas I, Finoia P, Williams GB, Allanson J, Pickard JD, Owen AM, Naci L, Menon DK, Stamatakis EA, 2019. Consciousness-specific dynamic interactions of brain integration and functional diversity. Nat Commun 10, 4616. [PubMed: 31601811]

Martin-Signes M, Perez-Serrano C, Chica AB, 2019. Causal Contributions of the SMA to Alertness and Consciousness Interactions. Cereb Cortex 29, 648–656. [PubMed: 29300881]

Mitra A, Snyder AZ, Tagliazucchi E, Laufs H, Raichle ME, 2015. Propagated infra-slow intrinsic brain activity reorganizes across wake and slow wave sleep. Elife 4.

Monti MM, Lutkenhoff ES, Rubinov M, Boveroux P, Vanhaudenhuyse A, Gosseries O, Bruno MA, Noirhomme Q, Boly M, Laureys S, 2013. Dynamic change of global and local information processing in propofol-induced loss and recovery of consciousness. PLoS Comput Biol 9, e1003271. [PubMed: 24146606]

Monti MM, Vanhaudenhuyse A, Coleman MR, Boly M, Pickard JD, Tshibanda L, Owen AM, Laureys S, 2010. Willful modulation of brain activity in disorders of consciousness. N Engl J Med 362, 579–589. [PubMed: 20130250]

Moon JY, Lee U, Blain-Moraes S, Mashour GA, 2015. General relationship of global topology, local dynamics, and directionality in large-scale brain networks. PLoS Comput Biol 11, e1004225. [PubMed: 25874700]

Norton L, Hutchison RM, Young GB, Lee DH, Sharpe MD, Mirsattari SM, 2012. Disruptions of functional connectivity in the default mode network of comatose patients. Neurology 78, 175–181. [PubMed: 22218274]

O'Regan JK, Noe A, 2001. A sensorimotor account of vision and visual consciousness. Behav Brain Sci 24, 939–973; discussion 973–1031. [PubMed: 12239892]

Owen AM, Coleman MR, Boly M, Davis MH, Laureys S, Pickard JD, 2006. Detecting awareness in the vegetative state. Science 313, 1402. [PubMed: 16959998]

Pan J, Xie Q, Qin P, Chen Y, He Y, Huang H, Wang F, Ni X, Cichocki A, Yu R, Li Y, 2020. Prognosis for patients with cognitive motor dissociation identified by brain-computer interface. Brain 143, 1177–1189. [PubMed: 32101603]

Power JD, Barnes KA, Snyder AZ, Schlaggar BL, Petersen SE, 2012. Spurious but systematic correlations in functional connectivity MRI networks arise from subject motion. Neuroimage 59, 2142–2154. [PubMed: 22019881]

Qin P, Di H, Liu Y, Yu S, Gong Q, Duncan N, Weng X, Laureys S, Northoff G, 2010. Anterior cingulate activity and the self in disorders of consciousness. Hum Brain Mapp 31, 1993–2002. [PubMed: 20336686]

Qin P, Wu X, Huang Z, Duncan NW, Tang W, Wolff A, Hu J, Gao L, Jin Y, Wu X, Zhang J, Lu L, Wu C, Qu X, Mao Y, Weng X, Zhang J, Northoff G, 2015. How are different neural networks related to consciousness? Ann Neurol 78, 594–605. [PubMed: 26290126]

Schiff ND, 2015. Cognitive Motor Dissociation Following Severe Brain Injuries. JAMA Neurol 72, 1413–1415. [PubMed: 26502348]

Seeley WW, Menon V, Schatzberg AF, Keller J, Glover GH, Kenna H, Reiss AL, Greicius MD, 2007. Dissociable intrinsic connectivity networks for salience processing and executive control. J Neurosci 27, 2349–2356. [PubMed: 17329432]

Siclari F, Baird B, Perogamvros L, Bernardi G, LaRocque JJ, Riedner B, Boly M, Postle BR, Tononi G, 2017. The neural correlates of dreaming. Nat Neurosci 20, 872–878. [PubMed: 28394322]

Stender J, Gosseries O, Bruno MA, Charland-Verville V, Vanhaudenhuyse A, Demertzi A, Chatelle C, Thonnard M, Thibaut A, Heine L, Soddu A, Boly M, Schnakers C, Gjedde A, Laureys S, 2014. Diagnostic precision of PET imaging and functional MRI in disorders of consciousness: a clinical validation study. Lancet 384, 514–522. [PubMed: 24746174]

Tagliazucchi E, Behrens M, Laufs H, 2013a. Sleep neuroimaging and models of consciousness. Front Psychol 4, 256. [PubMed: 23717291]

Tagliazucchi E, von Wegner F, Morzelewski A, Brodbeck V, Borisov S, Jahnke K, Laufs H, 2013b. Large-scale brain functional modularity is reflected in slow electroencephalographic rhythms across the human non-rapid eye movement sleep cycle. Neuroimage 70, 327–339. [PubMed: 23313420]

Tanabe S, Huang Z, Zhang J, Chen Y, Fogel S, Doyon J, Wu J, Xu J, Zhang J, Qin P, Wu X, Mao Y, Mashour GA, Hudetz AG, Northoff G, 2020. Altered Global Brain Signal during Physiologic, Pharmacologic, and Pathologic States of Unconsciousness in Humans and Rats. Anesthesiology 132, 1392–1406. [PubMed: 32205548]

Tang W, Liu H, Douw L, Kramer MA, Eden UT, Hamalainen MS, Stufflebeam SM, 2017. Dynamic connectivity modulates local activity in the core regions of the default-mode network. Proc Natl Acad Sci U S A 114, 9713–9718. [PubMed: 28827337]

Tononi G, Boly M, Massimini M, Koch C, 2016. Integrated information theory: from consciousness to its physical substrate. Nat Rev Neurosci 17, 450–461. [PubMed: 27225071]

Tsai PJ, Chen SC, Hsu CY, Wu CW, Wu YC, Hung CS, Yang AC, Liu PY, Biswal B, Lin CP, 2014. Local awakening: regional reorganizations of brain oscillations after sleep. Neuroimage 102 Pt 2, 894–903. [PubMed: 25067818]

van den Heuvel MP, Sporns O, 2013. Network hubs in the human brain. Trends Cogn Sci 17, 683–696. [PubMed: 24231140]

Vanhaudenhuyse A, Noirhomme Q, Tshibanda LJ, Bruno MA, Boveroux P, Schnakers C, Soddu A, Perlbarg V, Ledoux D, Brichant JF, Moonen G, Maquet P, Greicius MD, Laureys S, Boly M, 2010. Default network connectivity reflects the level of consciousness in non-communicative brain-damaged patients. Brain 133, 161–171. [PubMed: 20034928]

Windt JM, Nielsen T, Thompson E, 2016. Does Consciousness Disappear in Dreamless Sleep? Trends Cogn Sci 20, 871–882. [PubMed: 27765517]

Yan CG, Craddock RC, He Y, Milham MP, 2013. Addressing head motion dependencies for small-world topologies in functional connectomics. Front Hum Neurosci 7, 910. [PubMed: 24421764]

Yeo BT, Krienen FM, Sepulcre J, Sabuncu MR, Lashkari D, Hollinshead M, Roffman JL, Smoller JW, Zollei L, Polimeni JR, Fischl B, Liu H, Buckner RL, 2011. The organization of the human cerebral cortex estimated by intrinsic functional connectivity. J Neurophysiol 106, 1125–1165. [PubMed: 21653723]

Zhang J, Huang Z, Chen Y, Zhang J, Ghinda D, Nikolova Y, Wu J, Xu J, Bai W, Mao Y, Yang Z, Duncan N, Qin P, Wang H, Chen B, Weng X, Northoff G, 2018a. Breakdown in the temporal and spatial organization of spontaneous brain activity during general anesthesia. Hum Brain Mapp 39, 2035–2046. [PubMed: 29377435]

Zhang L, Luo L, Zhou Z, Xu K, Zhang L, Liu X, Tan X, Zhang J, Ye X, Gao J, Luo B, 2018b. Functional Connectivity of Anterior Insula Predicts Recovery of Patients With Disorders of Consciousness. Front Neurol 9, 1024. [PubMed: 30555407]

Highlight:

1. Adopt multiple altered conscious states to study neural correlates of consciousness
2. Sensorimotor cortex shows reduced degree centrality during unconsciousness
3. Connections between sensory and motor regions correlate with levels of consciousness

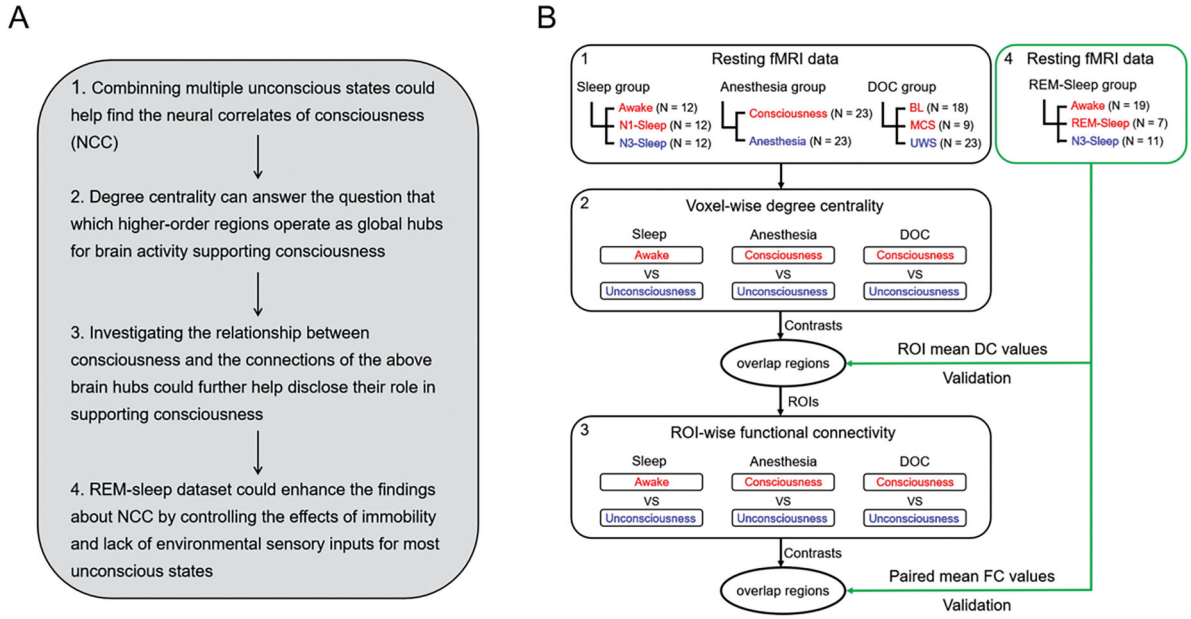

Fig. 1.

The schemata for experiment design and data processing. (A) The strategy of the experiment design and data analysis. (B) The schemata for experiment design. Red represents consciousness or reduced consciousness states; blue represents unconsciousness. The black square represents the exploratory datasets which were used to define the ROIs with degree centrality and functional connectivity changes during unconsciousness. The green square represents the validation datasets (REM-sleep group). DC values = degree centrality values, FC values = functional connectivity values. N: the sample size of each group. The digital number indicated the corresponding idea and data processing in panels A and B.

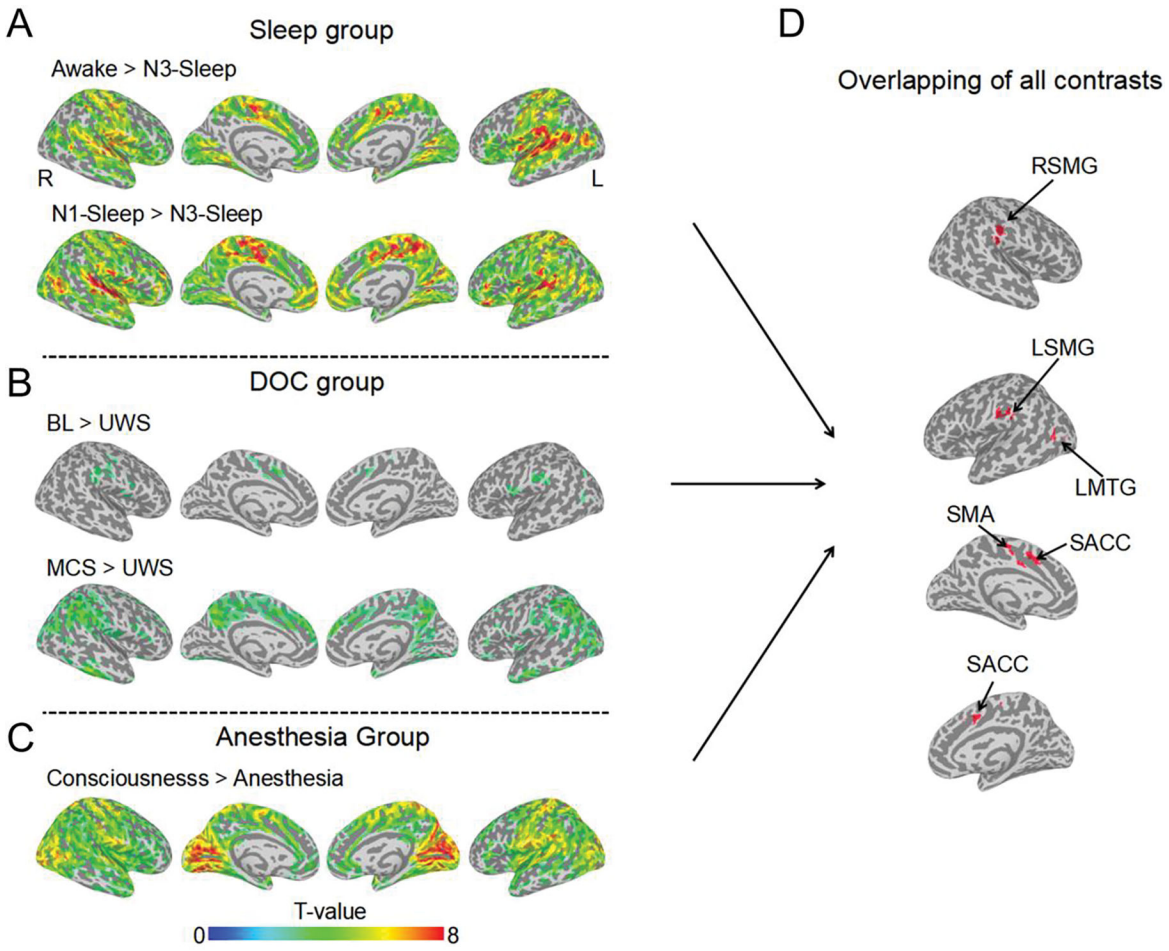

Fig. 2.

The brain regions with decreased degree centrality during unconsciousness. All the degree centrality contrasts for unconscious < conscious/reduced conscious states, (A) Sleep group, (B) DOC patient group and (C) anesthesia group. The activated clusters with ($p < 0.005$ uncorrected, volume > 20 voxels) are displayed. (D) The overlapped brain regions (volume > 20 voxels) of all the contrasts from panel A, B, and C. SMA = supplementary motor area; LSMG = left supramarginal gyrus; RSMG = right supramarginal gyrus; LMTG = left middle temporal gyrus; SACC = supragenual anterior cingulate cortex.

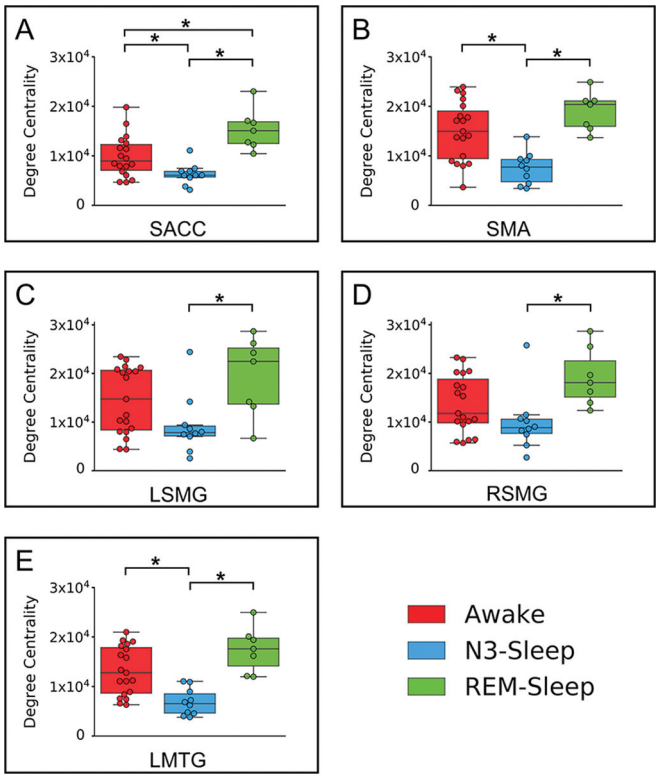

Fig. 3.

Degree centrality in REM-sleep group. The degree centrality (DC) values for awake, REM-sleep and N3-sleep states in SMA, SACC, LSMG, RSMG, and LMTG. (A) SACC: H(2) = 14.98, $\eta_H^2 = 0.41$, p < 0.001; post-hoc test showed N3-sleep < REM-sleep, p < 0.001, and N3-sleep < awake, p = 0.014. (B) SMA: H(2) = 14.01, $\eta_H^2 = 0.36$, p < 0.001; post-hoc test showed N3-sleep < REM-sleep, p = 0.001, and N3-sleep < awake, p = 0.003. (C) LSMG: H(2) = 6.94, $\eta_H^2 = 0.15$, p = 0.031; post-hoc test showed N3-sleep < REM-sleep, p = 0.014, and N3-sleep < awake, p = 0.085. (D) RSMG: H(2) = 8.53, $\eta_H^2 = 0.20$, p = 0.014; post-hoc test showed N3-sleep < REM-sleep, p = 0.007, and N3-sleep < awake, p = 0.089. (E) MTG:H(2) = 17.15, $\eta_H^2 = 0.46$, p < 0.001; post-hoc test showed N3-sleep < REM-sleep, p < 0.001, and N3-sleep < awake, p < 0.001. * means p < 0.05 FDR corrected.

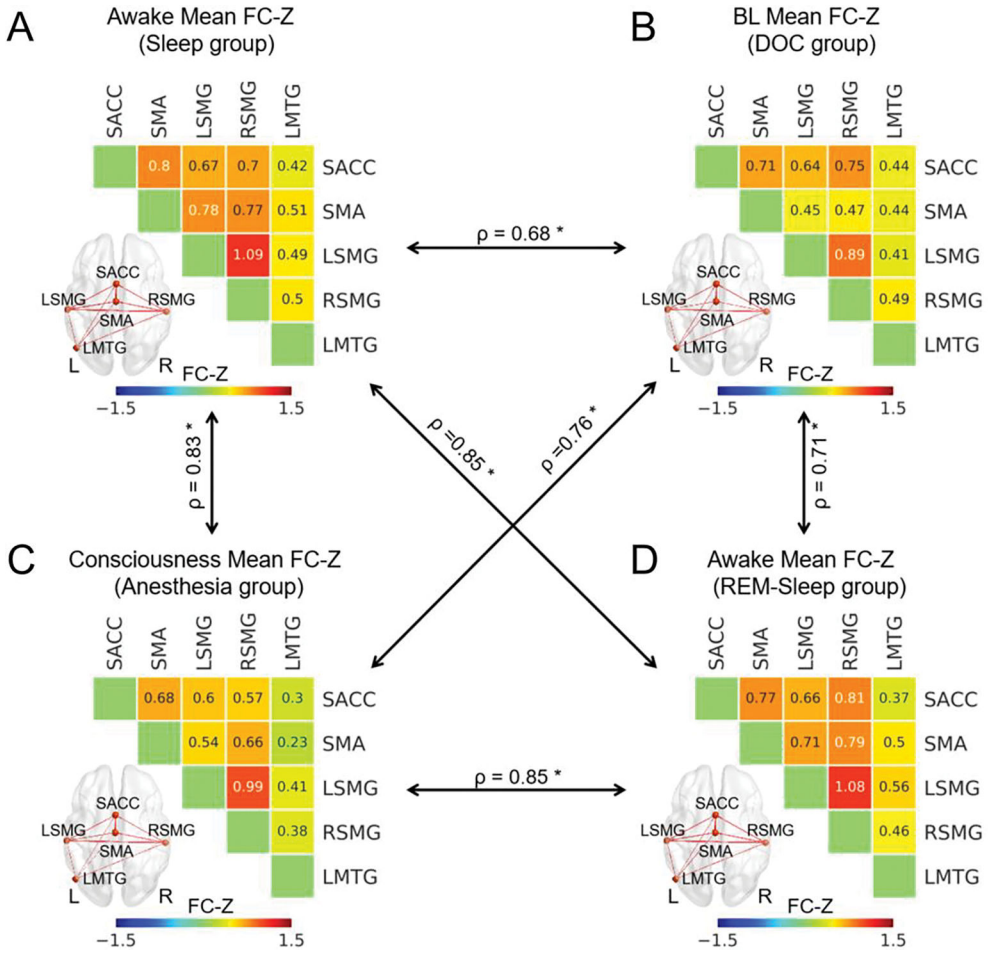

Fig. 4.

ROI-wise functional connectivity during consciousness in all four groups. The ROI-wise functional connectivity z-values for the awake-state in the sleep group (A), for BL patients in the DOC group (B), for the conscious state in the anesthesia group (C), and for the awake-states in the REM-sleep group (D). The black arrow represented the correlation of these functional connectivity between each pair of groups which was calculated through the Spearman's correlation. * means $p < 0.05$ FDR corrected. The thickness of lines in brain image represented the functional connectivity z-values between two states.

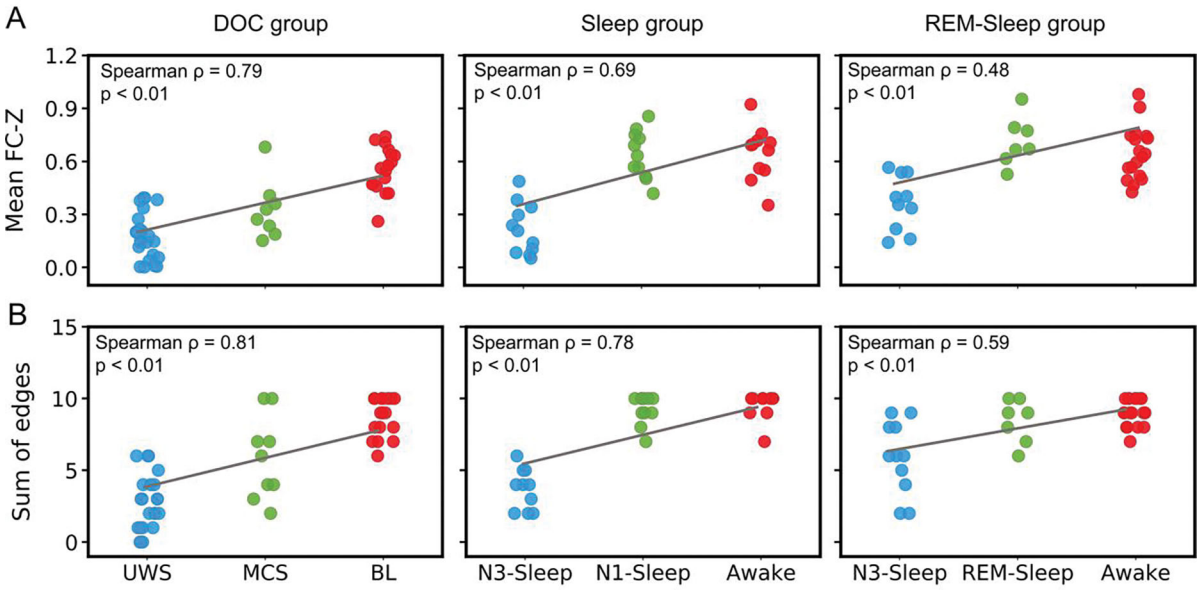

Fig. 5.

The relationship between functional connectivity and levels of consciousness. (A) The correlation between mean functional connectivity (FC) z-values (of all FCs among the five ROIs: SACC, SMA, LSMG, RSMG and LMTG) for each subject and consciousness states, in patients with DOC (left panel), sleep group (middle panel), and REM-sleep group (right panel). (B) The correlation between the sum of edges (of all FCs among the five ROIs: SACC, SMA, LSMG, RSMG and LMTG) and consciousness states, in patients with DOC (left panel), sleep group (middle panel), and REM-sleep group (right panel). Edge = one FC with Z value > 0.3095.

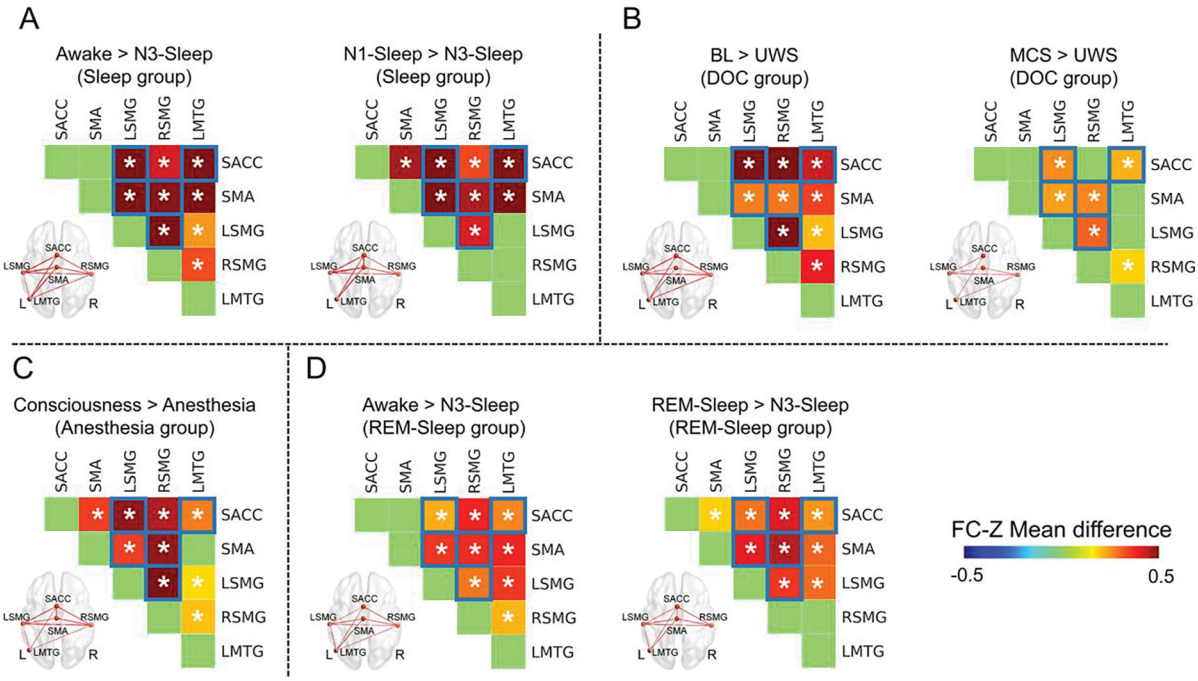

Fig. 6.

Reduced functional connectivity during unconsciousness. (A) Functional connectivity (FC) with significant reduction in the N3-sleep compared with awake and N1-sleep in the sleep group. (B) FC with a significant reduction in UWS compared with BL and MCS in the DOC group. (C) FC with a significant reduction in anesthesia compared with consciousness in the anesthesia group. (D) FC with significant reduction in N3-sleep compared with awake and REM-sleep in the REM-sleep group. * means $p < 0.05$, corrected. The functional connectivity marked with blue squares showed consistent reduction during unconsciousness in all four groups. The thickness of lines in brain image represented the difference of functional connectivity between two states.

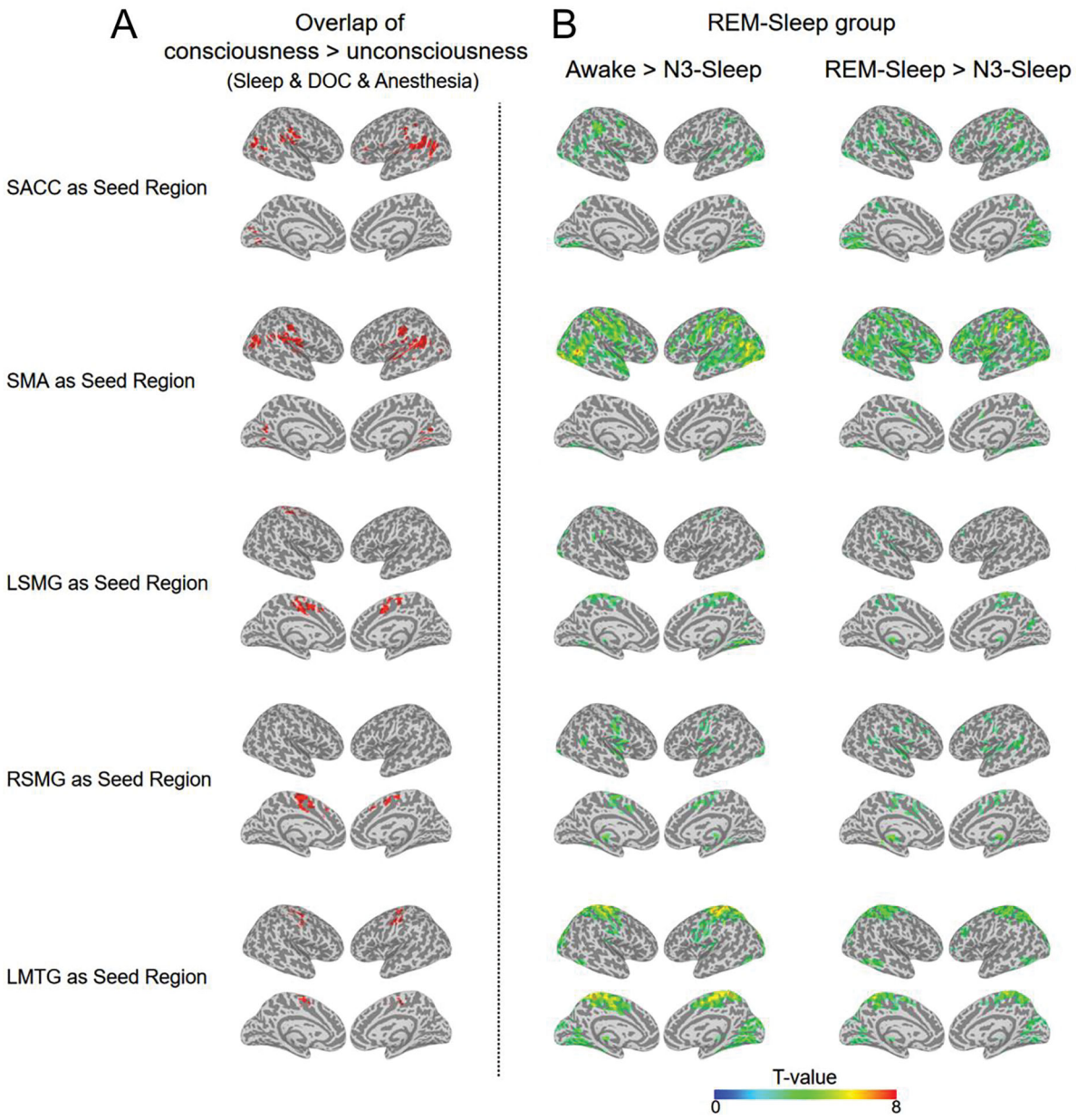

Fig.7.

voxel-wise functional connectivity in unconscious states. (A) For each seed region, the overlapped regions for all consciousness vs. unconsciousness contrasts (BL > UWS; MCS > UWS, awake > N3-sleep, N1-sleep > N3-sleep, and consciousness > anesthesia) (volume > 20 voxels). (B) In REM-sleep group, the voxel-wise FC contrasts: Awake > N3-sleep (the left panel) and REM-sleep > N3-sleep. The activation clusters are displayed ($p < 0.005$ uncorrected, volume > 20 voxels).